Journal of Molecular Catalysis A: Chemical 332 (2010) 122–127

Contents lists available at ScienceDirect

Journal of Molecular Catalysis A: Chemical

journal homepage: www.elsevier.com/locate/molcata

Structure and properties of tungsten peroxopolyoxo complexes – Promising catalysts for organics oxidation. I. Structure of peroxocomplexes studied during the stepwise synthesis of tetra(diperoxotungsten)phosphate-tetra-n-butyl ammonium

Zinaida P. Pai*, Dimitry I. Kochubey, Polina V. Berdnikova, Vladislav V. Kanazhevskiy, Irina Yu. Prikhod'ko, Yuriy A. Chesalov

Boreskov Institute of Catalysis, Siberian Branch of RAS, 630090 Novosibirsk, pr. Lavrentieva 5, Russia

ARTICLE INFO

Article history:
Received 4 June 2010
Received in revised form 27 August 2010
Accepted 4 September 2010
Available online 21 September 2010

Keywords:
Metal complex catalysis
Oxotungstates
Peroxopolyoxotungstates
EXAFS and Raman scattering spectroscopy
Oxidation of cyclic alkenes and alcohols

ABSTRACT

Catalysis via metal complexes has been studied using EXAFS and Raman spectroscopy. Main polyoxo- and peroxopolyoxocomplexes of tungsten, resulting from the interaction of phosphorus tungsten heteropolyacid with hydrogen peroxide in water solutions, were investigated with regard to their form and structure. Interaction was shown to reduce the nuclearity of forming complexes with respect to their precursor – $H_3PW_{12}O_{40}$. The symmetry of oxygen environment of tungsten was found to change, distances W–W remaining the same. After complex $[Bu^n_4N]_3\{PO_4[WO(O_2)_2]_4\}$ is isolated, binuclear anion $[W_2O_3(O_2)_4(H_2O)_2]^{2-}$ stays in the solution. Raman scattering, EXAFS and IR spectroscopy show that isolated peroxocomplex in its crystal state has four nuclei, and most probably retains this structure being dissolved in acetonitrile.

Synthesized catalytic complex $[Bu^n_4N]_3\{PO_4[WO(O_2)_2]_4\}$ was tested in oxidation of cyclic alkenes and alcohols with hydrogen peroxide. Complex $[Bu^n_4N]_3\{PO_4[WO(O_2)_2]_4\}$ was proved to provide higher yields of mono- and dicarbonic acids in comparison to *in situ* synthesized catalyst.

1. Introduction

In nowadays research the structure of dissolved complexes is still hard to access. Standard X-ray methods such as SAXS and diffuse scattering inform us about the size of particles and atomic spacing, respectively. Most often structure revealing methods are used to analyze solid crystal phases isolated from various solutions. However, a set of in series isolated phases allows one to judge about solution composition in total [1]. In practice, particularly in catalysis, the dissolved complex structure development in the reaction course remains the very important object of research. This problem is the key one for the homogeneous metal complex catalysis, including the one involving tungsten peroxocomplexes [2]. EXAFS spectroscopy is one of the recent advances used for the problem solution [3].

For quite a long time tungsten complexes are successfully used as catalysts for oxidizing various organic substrates by hydrogen peroxide water solutions in the two-phase systems (organic phase–aqueous phase): in 1959 Payne and Williams were the first to perform epoxidation of α,β-unsaturated acids by hydrogen peroxide, using sodium tungstate as catalyst precursor [4]. Since that time many processes for oxidizing organic compounds were developed, 10–35% aqueous H_2O_2 solutions acting as oxidizers in the presence of peroxocomplexes of tungsten *in situ* forming in systems H_2O_2 – H_3PO_4 – Na_2WO_4 [5], $H_3PW_{12}O_{40}$ – H_2O_2 [6] or H_2O_2 – Na_2WO_4 – $NH_2CH_3PO_3H_2$ [7]. Quaternary ammonium salts of chlorine, fluorine, bromine or hydrosulfate, containing $C_4 \div C_{18}$ alkyl groups or cations like $[C_5H_5N–C_{16}H_{33}]^+$, are applied as interphase transfer catalysts. It is well known that many catalytically active and inactive peroxopolyoxocomplexes of tungsten are *in situ* formed in the system. However, the structure of catalytically active complex is still an issue.

Many data obtained by various researchers in the field [5–9 and others] show that in solution such catalytic complexes most likely are in a poly-nuclear state, presumably in binuclear (W_2) or four-nuclear (W_4) one, depending on preparation conditions [6a,7a]. The ^{31}P with ^{183}W NMR spectroscopy indicated that a mixture of several anions: $[PWO_q]^{\delta-}$, $[PW_2O_p]^{\alpha-}$, $[PW_3O_n]^{\beta-}$, $[PW_4O_m]^{\gamma-}$ was formed in the system $H_3[PW_{12}O_{40}]\cdot yH_2O/H_2O_2$ *in situ* at ratio $[H_2O_2]/[W] = 7/1$ [9a]. The binuclear complex $(Bu^n_4N)_2[HPW_2O_{14}]$ was isolated and characterized by X-ray when synthesis was performed at increased phosphorous concentration achieved by

* Corresponding author. Tel.: +8 383 326 95 67; fax: +8 383 326 95 67.
E-mail address: zpai@catalysis.ru (Z.P. Pai).

1381-1169/$ – see front matter © 2010 Elsevier B.V. All rights reserved.
doi:10.1016/j.molcata.2010.09.007

addition of H_3PO_4 to this system. The IR and NMR spectra suggested that in general the structure is maintained in acetonitrile at room temperature. However changes of chemical shift in the ^{31}P with ^{183}W spectra of $(Bu^n_4N)_2[HPW_2O_{14}]$ solution show strong influence of solvation and interaction with cation $Bu^n_4N^+$ on local structure of $[HPW_2O_{14}]^{2-}$.

Individual four-nuclear complex was synthesized and isolated as crystal form by the authors of [6b], and its structure was characterized by the single crystal diffraction method. Unfortunately, not all structural data were published. Four-nuclear structure complexes may be also suggested regarding the data obtained for molybdenum peroxocomplex (see Fig. 1a) [10], whereas molybdenum is a chemical and crystal analog of tungsten. Structure data for anion $\{PO_4[MoO(O_2)_2]_4\}^{3-}$ were reported in detail. Therefore we are able to use them in the present study.

Earlier we optimized the conditions of synthesis and isolation of tungsten peroxocomplexes with different onium cations [13], which demonstrated high activity in organic substrates oxidation reactions [14].

In our work we used conditions in that mainly complex $[Bu^n_4N]_3\{PO_4[WO(O_2)_2]_4\}$ (**II**) must be produced and focused on the use of EXAFS combined with IR and Raman spectroscopy for accessing the state (local structure) of that tungsten peroxocomplex in reactive solutions. In contrast to work [9a] we investigated complex in solids and in reactive solutions without extracting one crystal form.

2. Experimental

For the study we used chemical grade $H_3PW_{12}O_{40}\cdot 6H_2O$ (**I**), chemical grade acetonitrile, $[Bu^n_4N]Cl$ (≥95% ≪Acros≫), 30–35% water solution of chemical grade H_2O_2. Cyclohexene, cyclooctene, octan-1-ol, benzyl alcohol and other reagents produced by «Reakhim» were of chemical purity grade.

Complex $[Bu^n_4N]_3\{PO_4[WO(O_2)_2]_4\}$ (**II**) was synthesized according to procedure described elsewhere [13]: A 35% H_2O_2 solution (8.2 mL, 84.50 mmol) was added to a solution of $H_3PW_{12}O_{40}\cdot 6H_2O$ (1.250 g, 0.42 mmol) in water (3 mL). The reaction mixture was stirred at room temperature for 0.5 h, and then the solution of $[Bu^n_4N]Cl$ (0.3250 g, 1.17 mmol) in 3 mL of water was added portionwise. The solid white precipitate was filtered off on a glass filter, washed with a small amount of water, and dried in air (yield: 0.6168 g, 77%). IR (cm^{-1}): 523, 549, 575, 591, 650, 845, 856, 972.

2.1. Physical–chemical studies

X-ray tungsten L_3-edge absorption spectra were registered at the EXAFS station of Synchrotron Radiation Center SB RAS (Novosibirsk) according to standard procedure [15]. The electrons energy in storage ring (VEPP-3) was 2 GeV, beam current being 80 mA. Spectrometer was equipped with cut-off two-crystal monochromator Si(1 1 1) and proportional chambers as detectors.

For all samples oscillation part of EXAFS-spectra ($\chi(k)$) was analyzed as $k^2\chi(k)$ in wave number range $k = 3.0–14\ Å^{-1}$. VIPER software was used to isolate the oscillation part of absorption coefficient and spectra simulation for structure analysis [16]. Quantum chemistry parameters for simulation were computed with software FEFF-7 [17].

For analysis solid samples were pressed to tablets with polypropylene (UHMW, Alfa Aesar) thickness enough to provide a tungsten content of 20 mg/cm^2. Solutions were poured into hermetic cells with polyethylene windows, tungsten concentration being 0.1 M.

In order to study how heteropolyacid (HPA) (**I**) interacts with the 30% aqueous solution of hydrogen peroxide with EXAFS we prepared samples (1–6), which model peroxocomplexes forming in reaction mixture at various synthesis stages:

Sample 1 (**I**) in crystal from (reference sample);
Sample 2 0.17 M aqueous solution of **I** (reference sample);
Sample 3 reaction mixture – aqueous solution of **I** with 30% aqueous solution of hydrogen peroxide, $[H_2O_2]/[H_3PW_{12}O_{40}] = 200$. Mixture was kept at room temperature being stirred for 30 min;
Sample 4 mother liquor (filtrate) after isolation of complex salt **II**;
Sample 5 complex **II** in crystal form;
Sample 6 0.025 M solution of complex **II** in acetonitrile.

For preparing samples 4 and 5 we stirred sample 3, portion by portion adding 0.65 g of $[Bu^n_4N]Cl$ preliminarily dissolved in 2 ml of water, then filtered crystal sediment over glass Shott filter, then washed it with cooled water (∼10 °C), and dried in air.

Raman spectra of solids and their solutions in a range of 100–3600 cm^{-1} were recorded using Raman-Fourier spectrometer RFS 100\S (Bruker); Nd-YAG laser ($\lambda = 1064$ nm, emission power 400 mWt) was used for excitation.

2.2. Catalytic oxidation of organic substrates

Selective catalytic oxidation of cycloalkenes and alcohols was performed in a cone flask equipped with a backflow condenser and magnetic stirrer (600 min^{-1}). Reaction temperature 80–90 °C was maintained with water thermostat with an accuracy of ±0.1 °C. Reaction mixture was prepared as follows: weighted catalyst sample was put into the flask, then substrate was added. After that reaction mixture was stirred, and 30% aqueous hydrogen peroxide was introduced. Then reaction mixture was heated up to required temperature. Substrates conversion was determined with GC (chromatograph "Kristall-2000", Russia, flame-ionization detector, metal column 3 m × 2 mm, 0.4% OV-225 with graphitized thermal soot, nitrogen as gas carrier, injection temperature 150 or 180 °C, column temperature 100 or 140 °C, detector temperature — 120 °C). Component concentration was determined with inner normalizing, measurement accuracy being 10 rel. %.

2.3. Carbonic acids isolation from reaction medium

For a quantitative isolation of adipic, cork and benzoic acids reaction mixture was cooled to the room temperature, then 30 ml of 10% $NaHCO_3$ solution were added. Mixture was transferred to separating funnel. After that 30 ml of CH_2Cl_2 were added, and mixture was stirred. Organic phase was separated from the aqueous one, and 2–3 times washed with saturated $NaHCO_3$ solution. Drop by drop HCl (1:1) was added to the aqueous phase to pH 3, then aqueous phase was kept for ∼10 h at 8–10 °C. Crystal precipitate was filtered, washed with a small amount of cool water (<5 °C) and dried in air.

n-Octanoic acid was extracted by CH_2Cl_2 (1 × 10 ml and 3 × 5 ml). Extract was dewatered in a bath, and oily product was dried in desiccator over $CaCl_2$ (n_D^{24} 1.4290).

Thus obtained carbonic acids were identified with IR-spectrometry. IR-spectra were recorded with FT-801 (≪SIMEX≫, Russia). Spectra well accorded with the ≪SADTLER≫ reference database.

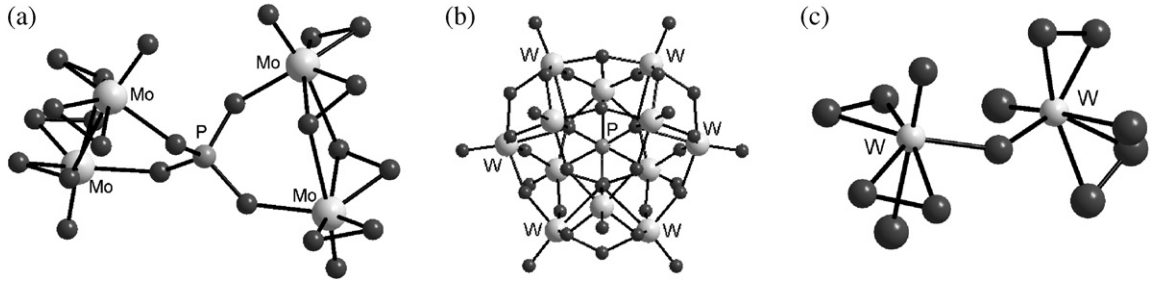

Fig. 1. Schematic view of anions (a) $\{PO_4[MoO(O_2)_2]_4\}^{3-}$ [10]; (b) $[PW_{12}O_{40}]^{3-}$ [11]; (c) $[W_2O_3(O_2)_4(H_2O)_2]^{2-}$ [12].

3. Results and discussion

3.1. Synthesis of catalytic complex *II*

In Fig. 2 one may see the curves of radial distribution of atoms (RDA) around W in samples 1–4. Let us note that sample 2 with dissolved oxometal complex **I** provides the widening of all peaks if compared to the solid sample 1 most likely due to the larger amplitude of thermal vibrations.

In whole, RDA curves comparison during the preparation of individual complex **II** allows us to suggest that when phosphorus-tungsten HPA (**I**) is used as synthesis precursor, it goes through two changes in its structure. First of all, nuclearity of complex with initial structure W_{12} (Fig. 1b) reduces, though distance W–W remains the same, being equal to ~3.6 Å. Secondly, the symmetry of oxygen environment of tungsten changes. In all cases there is one oxygen atom, which is linked to tungsten with a double bond (distance within 1.64–1.74 Å). There is also a group of distances within 1.9–2.0 Å. Both features are expressed on the RDA curves by well resolved peaks. However, distances within 1.9–2.0 Å merge into one peak due to the not enough sufficient method resolution. Peaks intensity changes owing to the changing symmetry of tungsten environment, total coordination number being constant and equal to six.

Questionable is the origin of peak around 3.3 Å. This peak characterizes all samples, and may be interpreted as distance W–O, but also as distance W–P. Let us note that bi-nuclear complex anions $[W_2O_{11}(H_2O)_2]^{2-}$ (W_2) contains at least two non equivalent tungsten atoms, which differ by their environment structure.

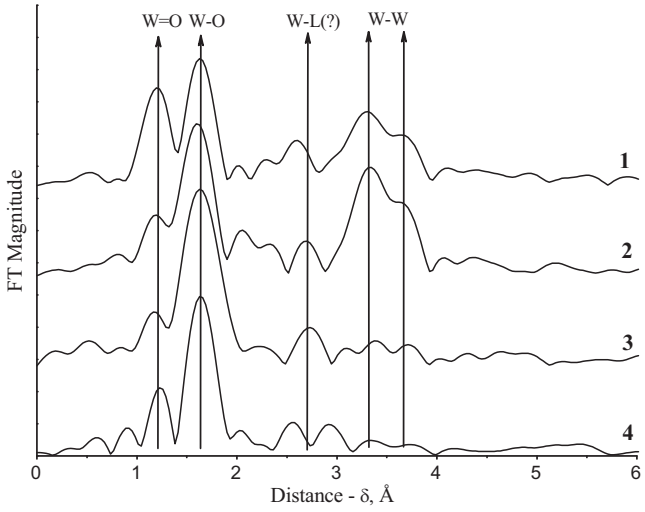

Fig. 2. Radial distribution of atoms around tungsten for samples: 1 – **I** in solid form; 2 – 0.17 M aqueous solution of **I**; 3 – reaction mixture (aqueous solution of I with 30% aqueous solution of hydrogen peroxide: $[H_2O_2]/[H_3PW_{12}O_{40}] = 200$; 4 – filtrate after isolation of salt $[Bu^n{}_4N]_3\{PO_4[WO(O_2)_2]_4\}$.

The solution of oxometallate **I** with H_2O_2 (sample 3) may contain both binuclear and more complex structure, resulting from the coordination of bi-nuclear particles with groups $[PO_4{}^{3-}]$ present in the solution. The fact, that various peroxocomplexes of tungsten differing by their composition may form and stay in equilibrium in the solution, was demonstrated by many researchers [7,8,13,18].

Since bi-nuclear complexes coordinated with $[PO_4]^{3-}$ groups appear to be mostly important for catalysis, we separated the forming complexes with the help of $[Bu^n{}_4N]Cl$. Thus we isolated complex **II** containing fragments with phosphorus, and then studied mother liquor (sample 4) in detail. Among all elements EXAFS revealed only tungsten and oxygen, and spectra were interpreted regarding this fact. Moreover, since position and shape of peak responsible for distance W–W in anion $[PW_{12}O_{40}]^{3-}$ remained the same, we decided that as attributed to sample 4 this peak is still responsible for distance W–W. EXAFS spectra simulations for sample 4 are given in Table 1.

If we compare experimental and simulated spectra (see Fig. 3), we see that chosen structure gives a well reproduced shape of peak in the range of interest. Simulation provided a set of coordination spheres with coordination numbers and interatomic distances given in Table 1. Apparently it is in a good agreement with the structure of bi-nuclear anion $[W_2O_3(O_2)_4(H_2O)_2]^{2-}$(Fig. 1c).

This result is also in accordance with the earlier obtained data [19], when during the synthesis of $[C_5H_5N(C_{16}H_{33})]_3\{PO_4[WO(O_2)_2]_4\}$ we took mother liquor, added KCl in excess and isolated the salt characterized by the IR spectrum (bands: 965, 952(shoulder), 835, 767, 616, 566, 552 cm^{-1}) referring to that of $K_2[W_2O_3(O_2)_4(H_2O)_2]\cdot 2H_2O$ according to studies [12,18,20].

3.2. Structure of complex *II*

We have studied the structure of isolated complex **II** in detail. Fig. 4 shows the RDA curves for complex **II** in solid state and for the same complex but dissolved in acetonitrile. Apparently, these curves coincide. Therefore, complex anion retains its local structure, when dissolving in acetonitrile in comparison with $(n\text{-}Bu_4N)_2[HPW_2O_{14}]$ complex studied in [9a]. Moreover, if we compare RDA curves obtained from the EXAFS spectra of complex **II** recorded immediately after dissolving and then in 9 h 45 min, we observe no significant changes in the oxygen environment of tungsten during this time.

Table 1
EXAFS spectra simulation for sample 4.

Coordination sphere	*R*, (Å)	N	σ^2, ($Å^{-2} \times 10^4$)	*R*-factor, (%)
W=O	1.75	1.6	45.0	23.2
W–O	1.96	4.0	34.9	
W–W	3.67	0.5	33.4	
W···H_2O_2 (solvated)	3.41	4.4	104.8	

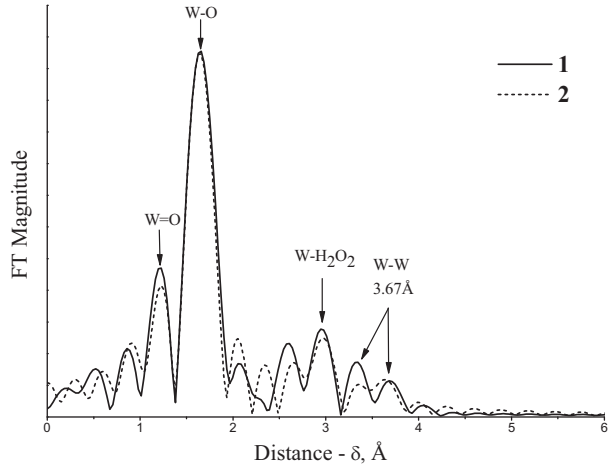

Fig. 3. Radial distribution of atoms around tungsten for sample **4**: 1 – experiment; 2 – simulation.

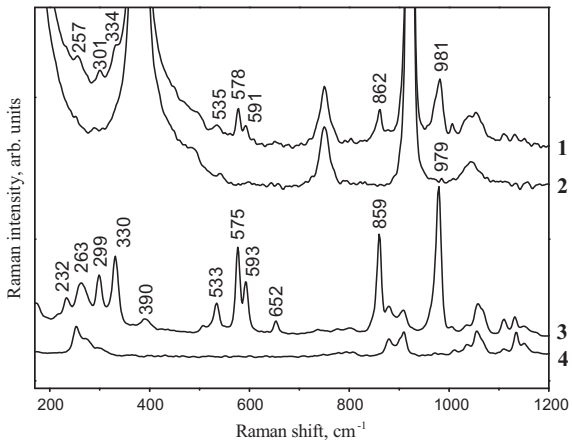

Fig. 5. Raman spectra: 0.025 M solution of complex **II** in acetonitrile (1), CH_3CN (2), solid complex **II** (3), solid $[Bu^n_4N]Cl$ (4).

Attribution of peaks on the RDA curves is similar to that described above except for the peak around 3.0 Å. According to [6b] in its solid form complex consists of two binuclear fragments $\{[WO(O_2)]_2(\eta^1,\eta^2\text{-}O_2)_2\}$, coordinated to phosphate $[\mu_4\text{-}PO_4]$, distance W–W inside the fragment being around 3.6 Å. Distance W–W marked in Fig. 3 was found to correspond to distance W–W equal to 3.6 Å with coordination number equal to unit, oxygen coordination number being equal to 6. Therefore, complex II indeed contains groups $\{[WO(O_2)]_2(\eta^1,\eta^2\text{-}O_2)_2\}$.

To be precise let us note that distance between the tungsten atoms in these binuclear fragments is about 6 Å, and thus is not observable by the EXAFS method. Therefore, let as pay attention to the peak marked in Fig. 4 as W–L, which may be attributed to distance W–P around 3.2–3.3 Å, thus being an evidence for the four-nuclear complex structure. Since the contribution of peaks from far distances is too small, accurate quantitative analysis is difficult. Distance W–L simulation as distance W–O results in negative coordination numbers, which have no physical sense. However, simulation as distance W–P gives inter-atomic distance 3.33 Å, which is similar to that in molybdenum complex [10], but with lower coordination number since structure disordering for this distance is not described by the Debye–Waller factor. This is also in a good agreement with the data of [6b], related to the similar complex structure, since in the latter distances W–P from different tungsten atoms differ by 0.1 Å, and their simulation by the mean distance fails to give real coordination numbers.

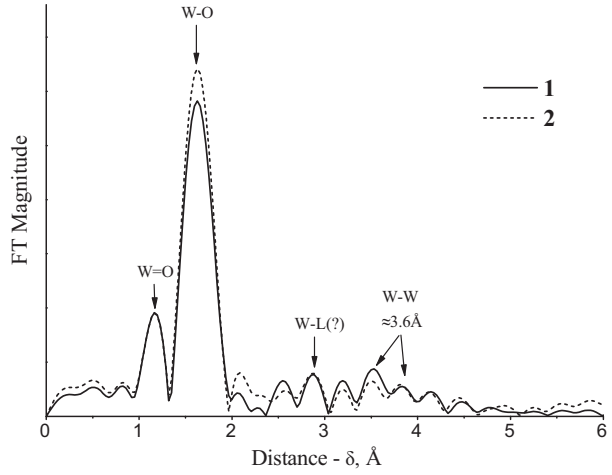

Fig. 4. Radial distribution of atoms around tungsten in catalytic complex **II**: 1 – solid form (sample 5); 2 – CH_3CN solution (sample 6).

Therefore, if we consider only EXAFS data, we may state that binuclear groups $\{[WO(O_2)]_2(\eta^1,\eta^2\text{-}O_2)_2\}$ are the main complex constituents. However, we are not able to say unambiguously that these groups coordinate around the phosphor atom forming the four-nuclear complex. Nevertheless, we may confirm the latter issue with the IR spectroscopy. According to [13], IR spectra of various peroxocomplexes differ considerably. Therefore, we may apply Raman spectroscopy to identify the structure of such complexes. Fig. 5 shows the spectra of complex **II** solid and dissolved in acetonitrile. Spectra of solid $[Bu^n_4N]Cl$ and pure acetonitrile are given for comparison.

Let us first consider the solid state complex. Beside the bands related to cation vibrations, its spectrum shows bands related to atomic vibrations in various peroxocomplex fragments: 979 (ν(W=O)), 859 (ν(O–O)), 652, 593, 575 and 533 (ν_{as}(W–(O_2)), ν_s(W–(O_2))), as well as 390, 330, 299, 263 и 232 cm^{-1}. The latter bands most likely reflect the deformations of complex fragments. Our spectrum practically coincides with the one of four-nuclear structure reported in [6b]. Unfortunately, Raman spectroscopy fails to register bands directly related to $\{PO_4\}$ vibrations due to their low intensity. These bands would have allowed us to understand unambiguously, if our complex is binuclear (W_2) or four-nuclear (W_4). Fortunately, in IR spectra bands related to vibrations of this particular fragment are strong enough [13]. In the IR spectra of the complex reported in [13] (it is characterized by identical Raman spectra, and we therefore take it for comparison) we observe bands 1085, 1052 и 1038 cm^1, attributed to vibrations $\nu_{as}(PO_4)$. Bands positions and number indicate that this complex contains fragment $\{PO_4\}$, its symmetry being lower than C_{3v}, which is in good agreement with the structure of anion $(\mu_4\text{-}PO_4)\{[WO(O_2)]_4(\eta^1,\eta^2\text{-}O_2)_4\}^{3-}$ suggested in [6b]. Let us note that we failed to analyze the IR spectrum of dissolved complex in a band range of 1100–1000 cm^{-1} due to the strong acetonitrile absorption. At the same time acetonitrile absorption in Raman spectra does not hinder the vibrations of complex **II** (Fig. 5). Bands positions and their relative intensities, as well as their number in the Raman spectra of complex solution in acetonitrile coincide with the same features of the solid state spectrum. Band shifts do not exceed 5 cm^{-1}, which may be explained by the difference of molecular interactions in acetonitrile solution and in solid state. Therefore, solid peroxocomplex **II** most likely retains its four-nuclear structure, when dissolving in acetonitrile.

Table 2
Catalytic oxidation of organic substrates to mono- and dicarbonic acids.

No	Substrate (sub)	T,°C	[Sub]/[Cat]	[Ox]/[Sub]	τ, h	Acid	Yield, %
1	Cyclohexene	92	200	4	2.5	Hexane-1,6-dioic (Adipic)	96–98
2	Cyclooctene	90	200	3	3	Octane-1,8-dioic (Cork)	85–87
3	Octan-1-ol	93	500	2	3	*n*-Octanoic (Caprylic)	60–65
4	Benzyl alcohol	90	500	3	4	Benzoic	82–85
5	Benzyl alcohol	90	500	2.5[a]	3	Benzoic	98–99

[a] H_2O_2 solution was dosed by three equal portions in 1 h each.

3.3. Testing of catalytic complex **II** in oxidation of organic substrates

Complex **II** was tested for its catalytic activity in the oxidative cleavage of C=C bond in cyclic alkenes yielding the corresponding dicarbonic acids, as well as in oxidation of alcohols yielding monocarbonic acids. A 30% solution of hydrogen peroxide in water served as oxidant (Ox). Reaction was performed in the two-phase system (organic phase–aqueous phase) with no organic solvents. Testing results are given in Table 2.

According to Table 2 at oxidation of cyclic alkenes in the presence of complex **II** the high yields of mono- and dicarbonic acids may be attained at temperatures 90–95 °C. During cyclohexene oxidation at 92 °C its conversion is almost 100%, and adipic acid yield attains 98% (Table 2, example 1), which is essentially higher than that given in [7b] (70% in 24 h), when catalyst was prepared *in situ*. Similar result was obtained at cyclooctene oxidation (Table 2, example 2), while in the presence of *in situ* prepared catalyst cork acid yield never exceeded 24% [7b]. This fact indirectly confirms the idea that, when catalyst is prepared *in situ* there is not only active complex **II** but also a less active tungsten complex, containing a binuclear anion $[W_2O_3(O_2)_4(H_2O)_2]^{2-}$, which we found in the mother liquor (sample 4). We may also suggest that complex containing anion $[W_2O_3(O_2)_4(H_2O)_2]^{2-}$ is easier to deactivate than complex **II**, which contains the stabilizing phosphate group.

Let us note that with above studied substrates it is necessary to have the excess of oxidant over stoichiometry. Example 3 in Table 2 shows that when oxidant to substrate ratio is close to reaction stoichiometry, product yield is low. Oxidant excess (see examples 1, 2, 4; Table 2) allows essentially higher product yields. We have already discussed this fact in our paper [12], and came to conclusion that it is possible to decrease the oxidant consumption using method suggested in [21]. Hydrogen peroxide addition portion by portion appears to be quite effective. In this case we can minimize the peroxide decomposition, and thus ratio [Ox]/[Sub] is close to stoichiometry, which is confirmed by example 5 in Table 2, showing a 98–99% yield of benzoic acid.

4. Conclusion

Our research in catalysis with metal peroxocomplexes using EXAFS and Raman spectroscopy revealed the structural features of polyoxo- and peroxopolyoxocomplexes of tungsten, forming as phosphorus tungsten HPA ($H_3PW_{12}O_{40}$) in aqueous solution interacts with the 30%-aqueous solution of H_2O_2. This interaction is shown to reduce the nuclearity of precursor, which initially has structure W_{12}. The symmetry of oxygen environment of tungsten is found to change, distances W–W remaining the same. After complex $[Bu^n_4N]_3\{PO_4[WO(O_2)_2]_4\}$ is isolated, binuclear anion stays in the aqueous phase $[W_2O_3(O_2)_4(H_2O)_2]^{2-}$.

EXAFS combined with Raman spectroscopy used to study local structure of the isolated complex in its solid state shows that it most likely has four-nuclear structure $[Bu^n_4N]_3\{PO_4[WO(O_2)_2]_4\}$, with the local structure near to structure of Venturello's complex [6a] which is retained, when complex is dissolved in acetonitrile. This complex has more rigid local structure as $(n\text{-}Bu_4N)_2[HPW_2O_{14}]$ [9a].

Synthesized catalytic complex $[Bu^n_4N]_3\{PO_4[WO(O_2)_2]_4\}$ was tested in the oxidation of cyclic alkenes and alcohols by hydrogen peroxide in two-phase systems (organic phase–aqueous phase) with no additional organic solvents. Apparently individual catalytic complex $[Bu^n_4N]_3\{PO_4[WO(O_2)_2]_4\}$ provides the higher yields of mono- and dicarbonic acids than *in situ* synthesized catalyst.

The next parts of this series of publications will be dedicated to changes of the local structure of catalysts depending on solvent polarity and in stoichiometric reactions.

Acknowledgements

The work was supported by Russian Foundation for Basic Research, Project 09-03-00395, and Department of Chemistry and Sciences on New Materials RAS, projects 5.7.3.

References

[1] M.M. Godneva, D.L. Motov, R.F. Okhrimenko, V.Ya. Kuznetsov, Zh. Neorg. Khim. 39 (1994) 740–742.
[2] J. Gao, Y. Chen, B. Han, Z. Feng, C. Li, N. Zhou, S. Gao, Z. Xi, J. Mol. Catal. A: Chem. 210 (2004) 197–204.
[3] (a) V.V. Kanazhevskii, V.P. Shmachkova, N.S. Kotsarenko, V.N. Kolomiichuk, D.I. Kochubei, J. Struct. Chem. 47 (2006) 860–868;
(b) O.V. Klimov, A.V. Pashigreva, D.I. Kochubei, G.A. Bukhtiyarova, A.S. Noskov, Dokl. Phys. Chem. 424 (2009) 497–501.
[4] G.B. Payne, P.H. Williams, J. Org. Chem. 24 (1959) 54–55.
[5] J.-M. Bregeault, M. Vennat, L. Salles, J.-Y. Piquemal, Y. Mahha, E. Briot, P.C. Bakala, A. Atlamsani, R. Thouvenot, J. Mol. Catal. A: Chem. 250 (2006) 177–189.
[6] (a) C. Venturello, E. Alneri, M. Ricci, J. Org. Chem. 48 (1983) 3831–3833;
(b) C. Venturello, R. D'Aloisio, J.C.J. Bart, M. Ricci, J. Mol. Catal. A: Chem. 32 (1985) 107–110;
(c) C. Venturello, M. Ricci, J. Org. Chem. 51 (1986) 1599–1602.
[7] (a) Y. Matoba, H. Inoue, J. Akagi, T. Okabayashi, Y. Ishii, M. Ogawa, Synth. Commun. 14 (1984) 865–873;
(b) Y. Ishii, K. Yamawaki, T. Ura, H. Yamada, T. Yoshida, M. Ogawa, J. Org. Chem. 53 (1988) 3587–3593;
(c) S. Sakaguchi, Y. Nishiyama, Y. Ishii, J. Org. Chem. 61 (1996) 5307–5311.
[8] R. Noyori, M. Aoki, K. Sato, Chem. Commun. (Cambridge, UK) 16 (2003) 1977–1988.
[9] (a) L. Salles, C. Aubry, R. Thouvenot, F. Robert, C. Doremieux-Morin, G. Chottard, H. Ledon, Y. Jeannin, J.-M. Bregeault, Inorg. Chem. 33 (1994) 871–878;
(b) Y. Mahha, L. Salles, J.-Y. Piquemal, E. Briot, A. Atlamsani, J.-M. Bregeault, J. Catal. 249 (2007) 338–348;
(c) L. Salles, R. Thouvenot, J.-M. Bregeault, Dalton Trans. (2004) 904–907.
[10] L. Salles, C. Aubry, R. Touvenot, F. Robert, G. Chottard, R. Thouvenot, H. Ledon, J.M. Bregeault, New J. Chem. 17 (1993) 367–375.
[11] J.F. Keggin, Proc. R. Soc. A 144 (1934) 75–100.
[12] F.W.B. Einstein, B.R. Penfold, Acta Cryst. 17 (1964) 1127–1133.
[13] Z.P. Pai, A.G. Tolstikov, P.V. Berdnikova, G.N. Kustova, T.B. Khlebnikova, N.V. Selivanova, A.B. Shangina, V.G. Kostrovskii, Russ. Chem. Bull. 54 (2005) 1847–1854.
[14] (a) Z.P. Pai, T.B. Khlebnikova, Y.V. Mattsat, V.N. Parmon, React. Kinet. Catal. Lett. 98 (2009) 1–8;
(b) Z.P. Khlebnikova, L.A. Pai, Y.V. Fedoseeva, T.B. Mattsat, React. Kinet. Catal. Lett. 98 (2009) 9–17.
[15] D.I. Kochubey, EXAFS Spectroscopy of Catalysts, Nauka, Novosibirsk, 1992.
[16] K.V. Klementev, Nucl. Instrum. Methods Phys. Res., Sect. A 448 (2000) 299–301.
[17] J.J. Rehr, A.L. Ankudinov, Radiat. Phys. Chem. 70 (2004) 453–463.

[18] C. Aubry, G. Chottard, N. Platzer, J.-M. Bregeault, R. Thouvenot, F. Chauveau, C. Huet, H. Ledon, Inorg. Chem. 30 (1991) 4409–4415.
[19] M.N. Timofeeva, Z.P. Pai, A.G. Tolstikov, G.N. Kustova, N.V. Selevanova, P.V. Berdnikova, K.P. Brylyakov, A.B. Shangina, V.A. Utkin, Russ. Chem. Bull. 52 (2003) 480–486.
[20] I.I. Vol'nov, Peroksokompleksy khroma, molibdena, vol'frama, Nauka, Moscow, 1989.
[21] B. Ying-li, Z. Mei-juan, H. Hong-yu, W. Chang-ping, L. Wen-xing, Z. Kai-ji, React. Kinet. Catal. Lett. 72 (2001) 73–82.